THE JOURNAL OF PHYSICAL CHEMISTRY LETTERS
A JOURNAL OF THE AMERICAN CHEMICAL SOCIETY

pubs.acs.org/JPCL

Letter

Observation of an Unusually Large IR Red-Shift in an Unconventional S−H···S Hydrogen-Bond

Kamal K. Mishra,[‖] Kshetrimayum Borish,[‖] Gulzar Singh, Prakash Panwaria, Surajit Metya, M. S. Madhusudhan,* and Aloke Das*

Cite This: *J. Phys. Chem. Lett.* 2021, 12, 1228−1235

Read Online

ACCESS | Metrics & More | Article Recommendations | Supporting Information

ABSTRACT: The S−H···S non-covalent interaction is generally known as an extremely unconventional weak hydrogen-bond in the literature. The present gas-phase spectroscopic investigation shows that the S−H···S hydrogen-bond can be as strong as any conventional hydrogen-bond in terms of the IR red-shift in the stretching frequency of the hydrogen-bond donor group. Herein, the strength of the S−H···S hydrogen-bond has been determined by measuring the red-shift (∼150 cm^{-1}) of the S−H stretching frequency in a model complex of 2-chlorothiophenol and dimethyl sulfide using isolated gas-phase IR spectroscopy coupled with quantum chemistry calculations. The observation of an unusually large IR red-shift in the S−H···S hydrogen-bond is explained in terms of the presence of a significant amount of charge-transfer interactions in addition to the usual electrostatic interactions. The existence of ∼750 S−H···S interactions between the cysteine and methionine residues in 642 protein structures determined from an extensive Protein Data Bank analysis also indicates that this interaction is important for the structures of proteins.

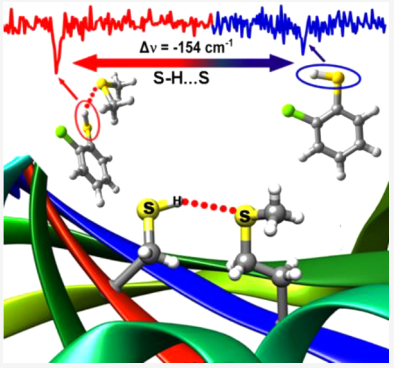

Despite a century of studies, the hydrogen-bond still fascinates the scientific community.[1] The importance of the hydrogen-bond interaction in biology, supramolecular chemistry, material science, etc. cannot be overemphasized.[2−5] A hydrogen-bond is generally denoted as X−H···Y, where X is a hydrogen-bond donor and Y is a hydrogen-bond acceptor atom or group. In a conventional hydrogen-bond, both the hydrogen-bond donor and acceptor atoms are strong in electronegativity. This type of hydrogen-bond is quite strong and stabilized mostly by the electrostatic interaction. On the other hand, either the hydrogen-bond acceptor or donor or even both the acceptor and donor atoms are weakly electronegative in the case of an unconventional hydrogen-bond. Indeed, there is a growing interest among researchers to search for the potential unconventional hydrogen-bonds involving various atoms in the periodic table following the redefinition of the hydrogen-bond by the IUPAC committee.[6] However, the physical nature, strength, and motif of the unconventional hydrogen-bonds are not understood well yet.

Recently, there have been several reports on understanding unconventional hydrogen-bonds involving less electronegative atoms (S, Se, P) as hydrogen-bond acceptors using gas-phase IR spectroscopy and quantum chemistry calculations.[7−21] However, most of the unconventional hydrogen-bonds reported in the literature deal with unconventional hydrogen-bond acceptor atoms, while the hydrogen-bond donor is still the conventional one, i.e., N−H, O−H, etc. On the other hand, detailed studies of the hydrogen-bonds involving an unconventional hydrogen-bond donor are mostly limited to C−H···Y hydrogen-bonds, where Y is generally a conventional hydrogen-bond acceptor (O, N, etc.), and this hydrogen-bond has been established as a weak non-covalent interaction.[3,22−24] Nevertheless, there are a few spectroscopic studies in the literature involving S as a hydrogen-bond donor with a π-electron cloud as well as N and O acting as hydrogen-bond acceptors.[25−31] These reports suggest that S, in general, is a weak hydrogen-bond donor as compared to N and O.

However, spectroscopic studies of an extremely unconventional hydrogen-bond (S−H···S) involving the less electronegative atom, S, as a hydrogen-bond donor as well as acceptor are sparse in the literature. It has been illustrated from a handful of solution-phase IR spectroscopic studies of particular molecular systems (i.e., diphenyl phosphinodithioic acid, thiolate salt, etc.) documented in the literature that the red-shift in the S−H stretching frequency for the S−H···S hydrogen-bond is quite large.[32,33] But quantitative information on the strength of the hydrogen-bond cannot be revealed in the solution phase due to intermolecular interaction with the solvent. Moreover, investigation of the S−H···S hydrogen-bond has not been further explored much in the literature, and this interaction is generally considered as a weak and rare hydrogen-bond. The only gas-phase report of microwave and

Received: October 20, 2020
Accepted: January 19, 2021
Published: January 25, 2021

https://dx.doi.org/10.1021/acs.jpclett.0c03183
J. Phys. Chem. Lett. 2021, 12, 1228−1235

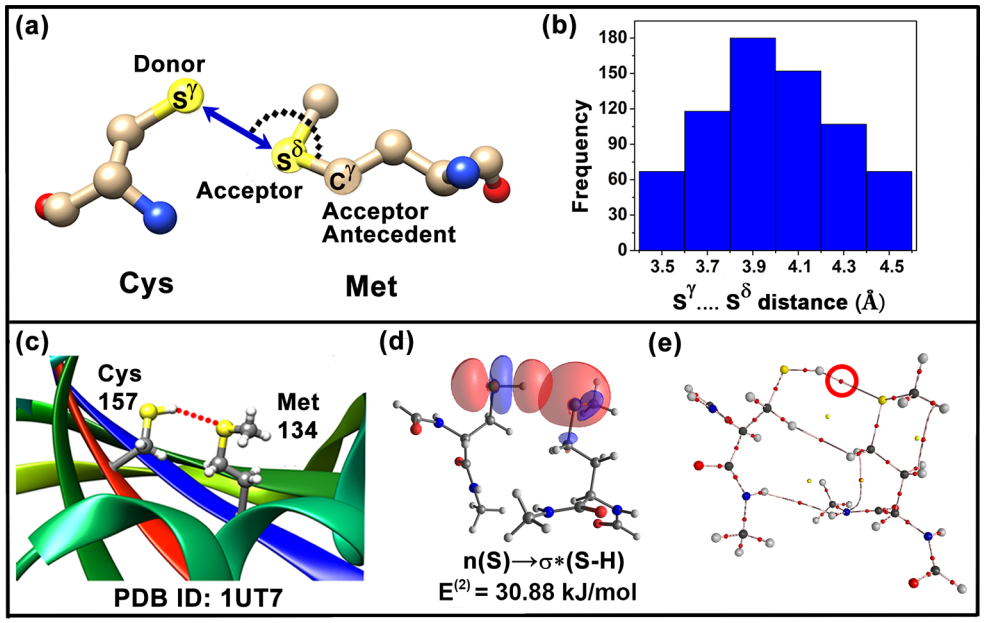

Figure 1. (a) Schematic diagram exhibiting the donor S^{γ} and acceptor S^{δ} atoms of Cys and Met, respectively. The acceptor antecedent atom is marked as C^{γ} in the Met residue. The $S^{\gamma}\cdots S^{\delta}$ distance and $\angle S^{\gamma}\cdots S^{\delta}-C^{\gamma}$ antecedent angle are the parameters used for searching S−H···S hydrogen-bonds in the PDB. (b) Histogram displaying the frequency of the S−H···S interactions in the PDB as a function of the $S^{\gamma}\cdots S^{\delta}$ distance. (c) A representative example of the S−H···S interaction in a protein (PDB ID: 1UT7). (d) NBO overlap for the S−H···S hydrogen-bond in the PDB structure (ID: 1UT7) following partial optimization of the hydrogen atoms of the interacting peptides in the protein. NBO second-order perturbation energy $[E^{(2)}]$ values are provided in the figure. (e) QTAIM analysis showing a molecular graph marking the bond critical point (BCP) for the S−H···S hydrogen-bond by a red circle in the crystal structure of the protein (PDB ID: 1UT7).

vacuum ultraviolet (VUV)-IR spectroscopy studies of H_2S dimer demonstrates that the IR red-shift in the hydrogen-bonded S−H stretching frequency compared to the free S−H frequency is 31 cm^{-1}, and thus, the S−H···S hydrogen-bond is found to be a weak interaction.[34,35] In general, the IR red-shift value in the vibrational frequency of the hydrogen-bond donor, as well as the enhancement of its intensity and broadening of the transition, is a measure of the strength of the hydrogen-bond.[36]

Apart from the limited spectroscopic studies, the very few X-ray crystallographic studies documented in the Cambridge Structural Database also reveal that S−H···S hydrogen-bonds are weak.[37−39] S−H···S hydrogen-bonds are also potential non-covalent interactions for the structures and functions of proteins and some other sulfur-containing biomolecules.[40,41] However, there are no detailed studies to determine the occurrence of the S−H···S interactions in proteins through a Protein Data Bank (PDB) analysis, probably due to the concept of the weak nature of this interaction.[42,43]

In this work, we have analyzed a total of 156 947 PDB structures to determine the occurrence of S−H···S hydrogen-bond interactions in proteins. Furthermore, we have studied a model complex of 2-chlorothiophenol (2-CTP) and dimethyl sulfide (Me_2S) using isolated gas-phase electronic and IR spectroscopy combined with quantum chemistry calculations to determine the intrinsic nature and strength of the S−H···S interaction.

Protein structures were downloaded from the RCSB PDB Web site.[44] Details of the PDB analysis are provided in the Supporting Information. Figure 1a displays a schematic diagram exhibiting the donor S^{γ} and acceptor S^{δ} atoms of cysteine (Cys) and methionine (Met) residues, respectively, in the proteins. The hydrogens were not added to the S^{γ} atoms of the Cys residues while using the REDUCE program to determine the hydrogen-bond angles, as we noticed that this program could not always optimize the positions of the hydrogen atoms to account for the S−H···S hydrogen-bonds in the crystal structures.[45] As an alternative, we considered the angle formed by the donor (S^{γ}), acceptor (S^{δ}), and acceptor antecedent (C^{γ}) atoms (Figure 1a), a well-known proxy for the hydrogen-bond angle when it is difficult to identify the hydrogen positions in the crystal structures.[46] Figure 1b shows a histogram representing the frequency of the S−H···S interactions as a function of the $S^{\gamma}\cdots S^{\delta}$ distance observed in the PDB. The cutoff for the antecedent angle $\angle S^{\gamma}\cdots S^{\delta}-C^{\gamma}$ was set between 90° and 180° as recommended by Baker et al.[46] The distance criterion for the S−H···S hydrogen-bond was chosen as 3.4 Å $\leq S^{\gamma}\cdots S^{\delta} \leq$ 4.6 Å. The maximum in the frequency of the S−H···S hydrogen-bond interactions appears at the $S^{\gamma}\cdots S^{\delta}$ distance of 3.8−4.0 Å, i.e., the H···S hydrogen-bond distance of 2.5−2.7 Å. Our PDB analysis shows that 642 protein structures have a total of 749 S−H···S hydrogen-bonds between the Cys and Met residues.

Figure 1c shows a representative example of the S−H···S interaction between the Cys and Met residues in a protein (PDB ID: 1UT7). The hydrogen atoms in the crystal structure shown in the figure are added using the REDUCE program to find the S−H···S hydrogen-bond (2.75 Å) and S···S (3.82 Å) distances in this protein. The short contact between the H and S atoms indicates attractive interactions between them. Further, we optimized quantum chemically only the hydrogen coordinates of the selected interacting peptides (Cys and Met residues) of the protein by keeping the coordinates of all other atoms fixed at the positions of the crystal structure. The S−H···S hydrogen-bond distance and ∠S−H···S angle in the partially optimized crystal structure obtained at the B97-D/6-311++G(d,p) level of theory are 2.53 Å and 158°, respectively. The presence of the S−H···S hydrogen-bond in the crystal structure

https://dx.doi.org/10.1021/acs.jpclett.0c03183
J. Phys. Chem. Lett. 2021, 12, 1228−1235

has been confirmed further through Natural Bond Orbital (NBO) and quantum theory of atoms in molecules (QTAIM) analyses of the partially optimized interacting units at the B97-D/6-311++G(d,p) level of theory. Figure 1d shows NBO overlap between the lone-pair orbital on the S atom of Met and the σ^* orbital of the S−H group of Cys. The NBO second-order perturbation energy $[E^{(2)}]$ for the donor−acceptor interaction is 30.88 kJ/mol. Figure 1e shows a molecular graph of the interacting units in the crystal structure obtained from the QTAIM analysis. There is a bond critical point (BCP) between the nonbonded H and S atoms with an electron density $[\rho(r)]$ value of 0.017 au. The Laplacian of the electron density $[\nabla^2\rho(r)]$ for the S−H···S hydrogen-bond is 0.035 au. Both the NBO and QTAIM results indicate that the S−H···S hydrogen-bond present in the crystal structure of the protein is quite strong.

However, it is important to note that the strength of the S−H···S hydrogen-bonds, i.e., the hydrogen-bond distances and angles, observed in different protein structures varies widely (Figure 1b) depending on the optimization of the local structures of the neighboring residues and other interactions present in the proteins. Thus, the intrinsic nature and strength of the S−H···S hydrogen-bond should be studied in the absence of any geometrical constraint and other significant interactions present in the system. We have explored a 1:1 model complex of 2-CTP and Me_2S (Figure 2b) using isolated gas-phase laser spectroscopy to probe the S−H···S interaction at the molecular level. We have studied the spectroscopy of the complex of 2-CTP instead of thiophenol, as the latter one has an extremely short lifetime in the excited electronic state.[47] Mass-selected electronic spectra of the *cis*-2-CTP monomer[47] and 1:1 2-CTP···Me_2S complex measured by one-color resonant two-photon ionization (1C-R2PI) spectroscopy are shown in Figure S1. The presence of two conformers of the 2-CTP···Me_2S complex, i.e., *cis*-2-CTP···Me_2S-1 and *trans*-2-CTP···Me_2S-1 (see the structures in Figure 2), is confirmed by UV−UV hole-burning spectroscopy (Figure S1c,d). A detailed description of the mass-selected electronic spectra of the 2-CTP monomer and its complexes with Me_2S is provided in the Supporting Information.

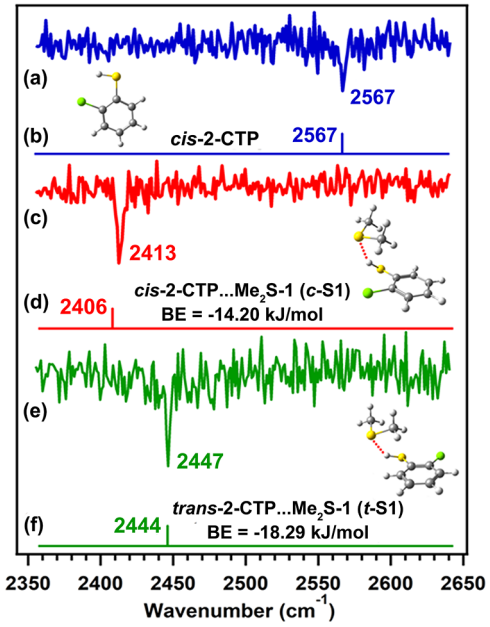

Figure 2. IR spectra of (a) *cis*-2-CTP, (c) *cis*-2-CTP···Me_2S, and (e) *trans*-2-CTP···Me_2S using RIDIR spectroscopy. (b), (d), and (f) are scaled theoretical IR spectra of *cis*-2-CTP, *cis*-2-CTP···Me_2S-1 (*c*-S1), and *trans*-2-CTP···Me_2S-1 (*t*-S1), respectively, calculated at the B97-D/6-311++G(d,p) level of theory.

Figure 2, panels a, c, and e, shows mass-selected conformation-specific IR spectra of the *cis*-2-CTP monomer, *cis*-2-CTP···Me_2S-1, and *trans*-2-CTP···Me_2S-1, respectively, measured in the S−H stretching region using resonant ion-dip infrared (RIDIR) spectroscopy. Detailed energetics and structural parameters of the *cis* and *trans* conformers of the 2-CTP monomer and 2-CTP···Me_2S complex obtained from calculations at the B97-D/6-311++G(d,p) level of theory are provided in Figures S2 and S3 and Tables S2 and S3. *cis*-2-CTP (Figure 2a) has a very weak S−H···Cl hydrogen-bond (∠S−H···Cl = 117°), which is absent in *trans*-2-CTP (Table S2 and Figure S2). The S−H···Cl hydrogen-bond becomes further weaker in the *cis*-2-CTP···Me_2S complex (∠S−H···Cl ≈ 101°), where the S−H group goes out of the plane by 40° (Table S2 and Figure S2). Each of the *cis*-2-CTP···Me_2S and *trans*-2-CTP···Me_2S complexes has two conformers. The higher energy conformers *cis*-2-CTP···Me_2S-2 (*c*-S2) and *trans*-2-CTP···Me_2S-2 (*t*-S2) shown in Figure S2 are almost isoenergetic with the corresponding lowest energy conformers *cis*-2-CTP···Me_2S-1 (*c*-S1) and *trans*-2-CTP···Me_2S-1 (*t*-S1) displayed in Figure 2. However, the *c*-S2 and *t*-S2 conformers are dispersion-dominated due to the orientation of the methyl groups of Me_2S toward the phenyl ring of 2-CTP, and the S−H···S hydrogen-bond present there is relatively weak (Figure S2). On the other hand, the lowest energy conformers *c*-S1 and *t*-S1 are dominated by hydrogen-bonding interactions. Interestingly, the S···S distance in the optimized structures of all the conformers of 2-CTP···Me_2S (3.8−3.9 Å, Table S2) is similar to that corresponding to the maximum number of S−H···S interactions found in the PDB.

Theoretical scaled S−H stretch frequencies of *cis*-2-CTP, *c*-S1, and *t*-S1 calculated at the B97-D/6-311++G(d,p) level of theory are provided as stick plots in Figure 2, panels b, d, and f, respectively. The S−H stretching frequency in the *cis*-2-CTP monomer appears at 2567 cm^{-1}. A scaling factor of 0.9712, obtained from the ratio of the experimental (2567 cm^{-1}) and theoretical (2643 cm^{-1}) S−H stretch frequencies of *cis*-2-CTP, has been employed to correct the harmonic S−H frequencies of the conformers of *cis*-2-CTP···Me_2S and *trans*-2-CTP···Me_2S calculated at the B97-D/6-311++G(d,p) level of theory (Table S4). There is a nice concurrence between the experimental and theoretical IR spectra of *c*-S1 and *t*-S1 presented in Figure 2. It could be noted that the S−H stretching frequency in *c*-S1 (2413 cm^{-1}) and *t*-S1 (2447 cm^{-1}) is red-shifted by 154 and 120 cm^{-1}, respectively, with respect to that in the *cis*-2-CTP monomer. Binding energies of *c*-S1 and *t*-S1 calculated at the B97-D/6-311++G(d,p) level of theory are −14.20 and −18.29 kJ/mol, respectively. The scaled S−H stretching frequencies in *c*-S2 and *t*-S2 calculated at the B97-D/6-311++G(d,p) level of theory are 2509 and 2506 cm^{-1} (Table S4), respectively, which are far away from the experimentally observed S−H stretching frequencies of the two conformers of the complex rendered in Figure 2. The conformers *c*-S2 and *t*-S2 are not observed in the experiment, probably due to conformational relaxation to their corresponding global minimum through a shallow potential energy barrier.[48]

https://dx.doi.org/10.1021/acs.jpclett.0c03183
J. Phys. Chem. Lett. 2021, 12, 1228−1235

The binding energies with and without thermal correction and S−H stretching frequencies of all the conformers of the 2-CTP···Me_2S complex have also been calculated at various other density functional theory (DFT) levels using different basis sets (Tables S3 and S4, Figure S3). A similar trend in the binding energies of the different conformers of the complex has been noticed at all the calculated levels of theory. It could be noted from Table S4 that the differences in the experimental S−H red-shift values of the *c*-S1 and *t*-S1 conformers are not reproduced well at various DFT levels, unlike the B97-D/6-311++G(d,p) level. However, all the theoretical levels of calculations demonstrate that the IR red-shift for the S−H···S hydrogen-bond is large. Furthermore, a similar red-shift in the S−H frequency in the conformers of the 2-CTP···Me_2S complex with respect to that in the *trans*-2-CTP monomer, without having any S−H···Cl hydrogen-bond, has been obtained from the theoretical calculation (Table S5). It is worth mentioning here that the theoretical red-shift values in the S−H stretching frequencies in the hydrogen-bond-dominated conformers of thiophenol (PhSH)···Me_2S and 4-chlorothiophenol (4-CTP)···Me_2S with respect to those in the PhSH and 4-CTP monomers calculated at the B97-D/6-311++G(d,p) level of theory are 132 and 145 cm^{-1}, respectively (Table S6). The result is quite enthralling, as the red-shift observed in the S−H stretching frequency for the S−H···S hydrogen-bond is similar to that reported for any conventional strong hydrogen-bond. Biswal and co-workers have reported a 130 cm^{-1} red-shift in the O−H stretching frequency for the O−H···S hydrogen-bond in a phenol···Me_2S complex.[49] Thus, the IR red-shifts for the S−H group are as high as those for conventional hydrogen-bond donors.

The strength of the S−H···S hydrogen-bond can further be compared with any conventional strong hydrogen-bond having both the hydrogen-bond donor and acceptor atoms strongly electronegative. The red-shift values in the X−H (X = O, N) stretching frequency reported for the N−H···O and O−H···O hydrogen-bonds in indole···H_2O and phenol···H_2O are 89 and 133 cm^{-1}, respectively.[50,51] Therefore, the S−H···S hydrogen-bond, despite being completely unconventional, is qualified as a strong hydrogen-bond like a conventional one. There is only one recent report of a gas-phase IR spectroscopy study of the S−H···S hydrogen-bond present in the H_2S dimer, which shows that the red-shift in the S−H stretching frequency is only 31 cm^{-1}; i.e., the S−H···S hydrogen-bond is weak.[35] The current results derived from the gas-phase IR spectroscopic study demonstrate for the first time that the S−H···S interaction can act as a strong hydrogen-bond.

We have also verified the strength of the S−H···S hydrogen-bond observed in the experiment by NBO and QTAIM analyses. NBO overlap between the lone-pair orbital on the S atom [n(S)] of Me_2S and the σ^* orbital of the S−H [σ^*(S−H)] of 2-CTP in *c*-S1 and *t*-S1 is provided in Figure S4, panels a and b, respectively. The second-order perturbation energy [$E^{(2)}$] values due to the interaction between the NBO donor and acceptor in *c*-S1 and *t*-S1 are 21.59 and 16.19 kJ/mol, respectively. Figure S4, panels c and d, shows molecular graphs of *c*-S1 and *t*-S1, respectively, obtained from AIM analysis performed at the B97-D/6-311++G(d,p) level of theory. BCPs between the S−H group of 2-CTP and the S atom of Me_2S with charge density [$\rho(r)$] of 0.015 and 0.014 au for *c*-S1 and *t*-S1, respectively, confirm the presence of a quite strong S−H···S hydrogen-bond. The Laplacians of the charge density [$\nabla^2\rho(r)$] values on the S−H···S hydrogen-bond in *c*-S1 and *t*-S1 are 0.032 and 0.031 au, respectively.

To find out the origin of the unusually large red-shift observed in the S−H stretching frequency of the S−H···S hydrogen-bond in the 2-CTP···Me_2S complex, the interaction energy was decomposed into different components using various energy decomposition analyses. Figure 3a shows energy

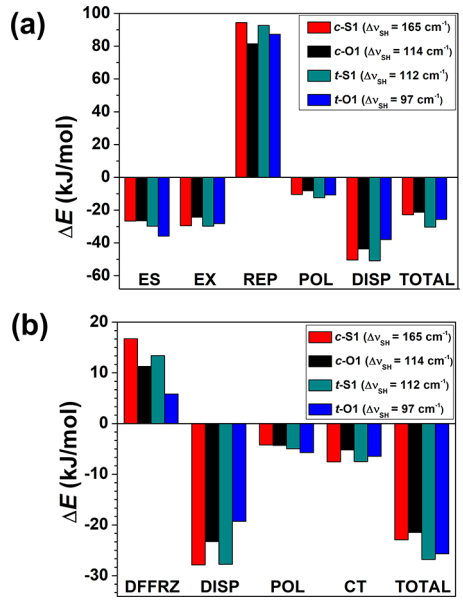

Figure 3. Decomposition of the interaction energies of the lowest energy *cis* and *trans* conformers of 2-CTP···Me_2S and 2-CTP···Me_2O using (a) LMO-EDA and (b) ALMO-EDA at the M06-2X/6-311++G(d,p) level of theory. In the LMO-EDA method, the components of the interaction energies are electrostatics (ES), exchange (EX), repulsion (REP), polarization (POL), and dispersion (DISP). The ALMO method decomposes the interaction energy into dispersion free frozen density (DFFRZ), dispersion (DISP), polarization (POL), and charge transfer (CT), where DFFRZ = electrostatics (ES) + Pauli repulsion (REP).

decomposition analysis (EDA) of the observed *cis* and *trans* conformers of the 2-CTP···Me_2S complex, i.e., *c*-S1 and *t*-S1, obtained by the localized molecular orbital energy decomposition analysis (LMO-EDA) method performed at the M06-2X/6-311++G(d,p) level of theory. EDA of the corresponding hydrogen-bonded conformers of 2-CTP···Me_2O, i.e., *cis*-2-CTP···Me_2O-1 (*c*-O1) and *trans*-2-CTP···Me_2O-1 (*t*-O1) (Figure S2), is also presented in Figure 3a for the comparison of the components of the interaction energy in the S−H···S and S−H···O bound complexes. The theoretical red-shift values in the S−H frequency ($\Delta\nu_{S-H}$) in these complexes are provided in the inset of Figure 3a. It is intriguing to note that the $\Delta\nu_{S-H}$ value for the S−H···S hydrogen-bond in *c*-S1 (165 cm^{-1}) is much larger than that for the S−H···O hydrogen-bond in *c*-O1 (114 cm^{-1}). However, the electrostatic (ES) interactions in both the S−H···S and S−H···O complexes are similar. In the case of the *trans* complexes, the $\Delta\nu_{S-H}$ value for the S−H···S hydrogen-bond in *t*-S1 (112 cm^{-1}) is also larger than that for the S−H···O hydrogen-bond in *t*-O1 (97 cm^{-1}), but the ES component in the former one is much smaller than that in the latter. Thus, the ES interaction is not sufficient to explain the origin of the atypical red-shifts observed in the S−H frequency due to the S−H···S hydrogen-bond interaction. Figure 3a also reveals that the dispersion (DISP) interaction in

https://dx.doi.org/10.1021/acs.jpclett.0c03183
J. Phys. Chem. Lett. 2021, 12, 1228−1235

both the *cis* and *trans* conformers of 2-CTP···Me_2S is more significant than that in those of 2-CTP···Me_2O, as S is more polarizable than O. However, it is reported that ES, charge-transfer (CT), and polarization components of the interaction energy contribute to the IR red-shift of the hydrogen-bond donor, whereas the DISP interaction contributes to the overall stabilization of the hydrogen-bonded complex.[52]

Absolutely localized molecular orbital energy decomposition analysis (ALMO-EDA) calculation has been performed to determine the CT component of the interaction energy in the complexes. It has been demonstrated recently that the second-generation ALMO-EDA method quite accurately determines the CT component of the interaction energy in the molecular complexes.[53,54] It is evident from Figure 3b that the CT component in both conformers of 2-CTP···Me_2S (*c*-S1 and *t*-S1) is much larger than that in the conformers of 2-CTP···Me_2O (*c*-O1 and *t*-O1) obtained from the ALMO-EDA calculation performed at the M06-2X/6-311++G(d,p) level of theory. A similar trend in the CT component of the interaction energies has been noticed from the ALMO-EDA calculations of 2-CTP···Me_2S and 2-CTP···Me_2O carried out at various levels of DFT (Figure S5). It is also captivating that the CT contribution to the strong S−H···S hydrogen-bond present in the *c*-S1 ($\Delta\nu_{S-H}$ = 165 cm^{-1}) and *t*-S1 ($\Delta\nu_{S-H}$ = 112 cm^{-1}) conformers is larger than that to the weak S−H···S hydrogen-bond present in the *c*-S2 ($\Delta\nu_{S-H}$ = 60 cm^{-1}) and *t*-S2 ($\Delta\nu_{S-H}$ = 48 cm^{-1}) conformers (Figure S6).

Further, Frontier Molecular Orbital (FMO) calculations have been performed at the B97-D/6-311++G(d,p) level of theory to determine the energy gap between the orbitals involved in the S−H···S and S−H···O interactions in the 2-CTP···Me_2S and 2-CTP···Me_2O complexes, respectively. The values of the energy gap between the HOMO of the lone-pair electrons (s and p types) on sulfur as well as oxygen atoms and the LUMO of the S−H antibonding orbital [σ^*(S−H)] in the lowest energy conformers of the 2-CTP···Me_2S and 2-CTP···Me_2O complexes (*c*-S1 versus *c*-O1 and *t*-S1 versus *t*-O1) at a very large intermolecular distance are provided in Table 1. The

Table 1. Energy Gap between the HOMO of the s and p Type Lone-Pair Electrons (n_p and n_s) on the Sulfur and Oxygen Atoms and LUMO of the S−H Antibonding Orbital [σ^*(S−H)] in the Lowest Energy *cis* and *trans* Conformers of the 2-CTP···Me_2S and 2-CTP···Me_2O Complexes at a Large Intermolecular Separation along the Hydrogen-Bond Coordinate Determined from Frontier Molecular Orbital Calculation Performed at the B97-D/6-311++G(d,p) Level of Theory

	HOMO−LUMO energy gap (eV)	
complex	n_p-σ^* (S−H)	n_s-σ^* (S−H)
c-S1	4.49	6.99
c-O1	5.33	7.06
t-S1	4.50	6.99
t-O1	5.40	7.03

FMO calculations point out that the HOMO−LUMO energy gap between the interacting molecular orbitals is smaller for the S−H···S hydrogen-bond compared to that for the S−H···O hydrogen-bond, and hence the orbital/CT interaction is stronger in the former with respect to the latter one. A similar trend in the HOMO−LUMO energy gap has been found from the FMO calculations of these two complexes performed at different levels of theory (Table S7).

The significance of the CT/orbital interaction in stabilizing various non-covalent interactions, including strong/weak hydrogen-bonds, has been demonstrated earlier through FMO calculations.[55] The HOMO−LUMO energy gap has also been compared with the energy difference between the NBO donor−acceptor orbitals involved in the S−H···S hydrogen-bond, and the trend is similar (Table S8). Thus, the ALMO-EDA, FMO, and NBO calculations reveal that the enhanced CT/orbital interaction found in the S−H···S hydrogen-bond compared to that in the S−H···O hydrogen-bond could have an important contribution to the unusually large red-shift observed in the S−H stretching frequency in the former one, containing less electronegative hydrogen-bond donor as well as acceptor atoms.

In summary, we have studied an extremely unconventional hydrogen-bond involving sulfur as a hydrogen-bond donor as well as an acceptor employing detailed PDB analysis, isolated gas-phase spectroscopy, and quantum chemistry calculations. PDB analysis reveals a total of 749 S−H···S interactions between the cysteine and methionine residues in 642 protein structures. A gas-phase IR spectroscopy study of the S−H···S hydrogen-bond in a model complex formed between 2-CTP and Me_2S reveals, for the first time, an unusually large red-shift (∼120−150 cm^{-1}) in the S−H stretching frequency. The strong S−H···S hydrogen-bond elucidated from the IR red-shift measured in the present work cannot be explained in terms of the conventional wisdom as an ES interaction, as S is a very weak electronegative atom. ALMO-EDA and FMO calculations of 2-CTP···Me_2S and 2-CTP···Me_2O demonstrate that the larger CT/orbital interaction in the S−H···S hydrogen-bond in comparison to the S−H···O contributes significantly to the IR red-shift of the S−H frequency in addition to the ES and polarization interactions. A comprehensive understanding of the unconventional but strong S−H···S hydrogen-bond in terms of the IR red-shift unveiled from the present investigation is extremely important for designing supramolecular assemblies and drugs containing S atoms. The current finding in this work will stimulate experimentalists as well as theoreticians to explore further the nature, physical origin, and strength of this unconventional but important S−H···S hydrogen-bond interaction. Specifically, matrix isolation FT-IR or Jet-FTIR spectroscopy will be very useful to study various thiophenol derivatives, as these techniques are not dependent on the lifetime of the electronically excited states.

EXPERIMENTAL METHODS

Experimental and theoretical methods were described in detail elsewhere and provided in the Supporting Information as well.[56,57] In brief, a mixed vapor of 2-chlorothiophenol (2-CTP, Sigma-Aldrich, 99%) heated at 70 °C and dimethyl sulfide (Me_2S, Sigma-Aldrich, ≥ 99%) kept in dry ice at −78 °C was seeded in a He−Ne (30:70) gas mixture (2.5 bar) and expanded through an orifice of a pulse solenoid valve (General Valve, 10 Hz, Series 9, 0.5 mm orifice diameter) into a high-vacuum chamber. A jet-cooled molecular beam of the complex was ionized by one-color resonant two-photon ionization (1C-R2PI) technique using an Nd:YAG pumped tunable dye laser (10 Hz, 10 ns). UV−UV hole-burning spectroscopy was used to discriminate the presence of different conformers in the experiment.[58] Mass-selected conformation-specific IR spectra

https://dx.doi.org/10.1021/acs.jpclett.0c03183
J. Phys. Chem. Lett. 2021, 12, 1228−1235

of the complex were measured by resonant ion-dip infrared (RIDIR) spectroscopy. Interpretation of the experimental results was done by performing quantum chemistry calculations using the Gaussian09 program package.[59] Binding energies of the complexes were corrected for the zero-point energy (ZPE) and basis set superposition error (BSSE).[60] Natural Bond Orbital (NBO)[61] analysis was done using the NBO6.0 program,[62] while the quantum theory of atoms in molecules (QTAIM) calculations[63] were performed using the AIM2000 program package.[64] Binding energies of the complexes were decomposed using localized molecular orbital energy decomposition analysis (LMO-EDA)[65] and second-generation absolutely localized molecular orbital energy decomposition analysis (ALMO-EDA)[53,54,66,67] implemented in the GAMESS-USA and Q-Chem5.3 packages, respectively.[68,69]

■ ASSOCIATED CONTENT

Supporting Information

The Supporting Information is available free of charge at https://pubs.acs.org/doi/10.1021/acs.jpclett.0c03183.

Detailed description of PDB analysis, experimental methods, 1C-R2PI and UV−UV hole-burning spectra, detailed results of computational investigation, Cartesian coordinates of the optimized structures, and list of the PDB IDs, including Figures S1−S6 and Tables S1−S8 (PDF)

■ AUTHOR INFORMATION

Corresponding Authors

M. S. Madhusudhan − *Department of Biology, Indian Institute of Science Education and Research Pune, Pashan, Pune 411008, India;* orcid.org/0000-0002-2889-5884; Email: madhusudhan@iiserpune.ac.in

Aloke Das − *Department of Chemistry, Indian Institute of Science Education and Research Pune, Pashan, Pune 411008, India;* orcid.org/0000-0002-2124-0631; Email: a.das@iiserpune.ac.in

Authors

Kamal K. Mishra − *Department of Chemistry, Indian Institute of Science Education and Research Pune, Pashan, Pune 411008, India*

Kshetrimayum Borish − *Department of Chemistry, Indian Institute of Science Education and Research Pune, Pashan, Pune 411008, India*

Gulzar Singh − *Department of Biology, Indian Institute of Science Education and Research Pune, Pashan, Pune 411008, India*

Prakash Panwaria − *Department of Chemistry, Indian Institute of Science Education and Research Pune, Pashan, Pune 411008, India*

Surajit Metya − *Department of Chemistry, Indian Institute of Science Education and Research Pune, Pashan, Pune 411008, India*

Complete contact information is available at: https://pubs.acs.org/10.1021/acs.jpclett.0c03183

Author Contributions

‖K.K.M. and K.B. contributed equally to this work.

Notes

The authors declare no competing financial interest.

■ ACKNOWLEDGMENTS

The financial support received from IISER Pune and SERB, India (Grant No. EMR/2015/000486), to perform this research is gratefully acknowledged. The computational support and resources provided by the "PARAM Brahma Facility" under the National Supercomputing Mission, Government of India at IISER, Pune, are also acknowledged. The authors would like to thank Dr. Biplab Sarkar at North-Eastern Hill University, Shillong, for helping us with some of the ALMO-EDA calculations using QChem5.3 software.

■ REFERENCES

(1) Latimer, W. M.; Rodebush, W. H. Polarity and ionization from the standpoint of the Lewis theory of valence. *J. Am. Chem. Soc.* **1920**, *42*, 1419−1433.

(2) Jeffrey, G. A.; Saenger, W. *Hydrogen Bonding in Biological Structures*; Springer: Berlin, 1991.

(3) Desiraju, G. R.; Steiner, T. *The Weak Hydrogen Bond in Structural Chemistry and Biology*; Oxford University Press: New York, 1999.

(4) Karshikoff, A. *Non-covalent Interactions in Proteins*; Imperial College Press: London, 2006.

(5) Lehn, J.-M. *Supramolecular Chemistry: Concepts and Perspectives*; John Wiley & Sons: New York, 1996.

(6) Arunan, E.; et al. Defining the hydrogen bond: An account (IUPAC Technical Report). *Pure Appl. Chem.* **2011**, *83*, 1619−1636.

(7) Chand, A.; Sahoo, D. K.; Rana, A.; Jena, S.; Biswal, H. S. The Prodigious Hydrogen Bonds with Sulfur and Selenium in Molecular Assemblies, Structural Biology, and Functional Materials. *Acc. Chem. Res.* **2020**, *53*, 1580−1592.

(8) Chand, A.; Biswal, H. S. Hydrogen Bonds with Chalcogens: Looking Beyond the Second Row of the Periodic Table. *J. Indian Inst. Sci.* **2020**, *100*, 77−100.

(9) Biswal, H. S.; Bhattacharyya, S.; Bhattacherjee, A.; Wategaonkar, S. Nature and strength of sulfur-centred hydrogen bonds: laser spectroscopic investigations in the gas phase and quantum-chemical calculations. *Int. Rev. Phys. Chem.* **2015**, *34*, 99−160.

(10) Biswal, H. S.; Wategaonkar, S. Nature of the N-H···S Hydrogen Bond. *J. Phys. Chem. A* **2009**, *113*, 12763−12773.

(11) Biswal, H. S.; Gloaguen, E.; Loquais, Y.; Tardivel, B.; Mons, M. Strength of NH···S Hydrogen Bonds in Methionine Residues Revealed by Gas-Phase IR/UV Spectroscopy. *J. Phys. Chem. Lett.* **2012**, *3*, 755−759.

(12) Mundlapati, V. R.; Sahoo, D. K.; Ghosh, S.; Purame, U. K.; Pandey, S.; Acharya, R.; Pal, N.; Tiwari, P.; Biswal, H. S. Spectroscopic Evidences for Strong Hydrogen Bonds with Selenomethionine in Proteins. *J. Phys. Chem. Lett.* **2017**, *8*, 794−800.

(13) Mishra, K. K.; Singh, S. K.; Ghosh, P.; Ghosh, D.; Das, A. The nature of selenium hydrogen bonding: gas phase spectroscopy and quantum chemistry calculations. *Phys. Chem. Chem. Phys.* **2017**, *19*, 24179−24187.

(14) Mishra, K. K.; Singh, S. K.; Kumar, S.; Singh, G.; Sarkar, B.; Madhusudhan, M. S.; Das, A. Water-Mediated Selenium Hydrogen-Bonding in Proteins: PDB Analysis and Gas-Phase Spectroscopy of Model Complexes. *J. Phys. Chem. A* **2019**, *123*, 5995−6002.

(15) Andersen, C. L.; Jensen, C. S.; Mackeprang, K.; Du, L.; Jørgensen, S.; Kjaergaard, H. G. Similar Strength of the NH···O and NH···S Hydrogen Bonds in Binary Complexes. *J. Phys. Chem. A* **2014**, *118*, 11074−11082.

(16) Hansen, A. S.; Vogt, E.; Kjaergaard, H. G. Gibbs energy of complex formation - combining infrared spectroscopy and vibrational theory. *Int. Rev. Phys. Chem.* **2019**, *38*, 115−148.

(17) Juanes, M.; Lesarri, A.; Pinacho, R.; Charro, E.; Rubio, J. E.; Enriquez, L.; Jaraiz, M. Sulfur Hydrogen Bonding in Isolated Monohydrates: Furfuryl Mercaptan versus Furfuryl Alcohol. *Chem. - Eur. J.* **2018**, *24*, 6564−6571.

(18) Juanes, M.; Saragi, R. T.; Caminati, W.; Lesarri, A. The Hydrogen Bond and Beyond: Perspectives for Rotational Investigations of Non-Covalent Interactions. *Chem. - Eur. J.* **2019**, *25*, 11402−11411.
(19) Du, L.; Tang, S.; Hansen, A. S.; Frandsen, B. N.; Maroun, Z.; Kjaergaard, H. G. Subtle differences in the hydrogen bonding of alcohol to divalent oxygen and sulfur. *Chem. Phys. Lett.* **2017**, *667*, 146−153.
(20) Hansen, A. S.; Du, L.; Kjaergaard, H. G. Positively Charged Phosphorus as a Hydrogen Bond Acceptor. *J. Phys. Chem. Lett.* **2014**, *5*, 4225−4231.
(21) Ghosh, S.; Chopra, P.; Wategaonkar, S. C-H···S Interaction Exhibits all the Characteristics of Conventional Hydrogen Bonds. *Phys. Chem. Chem. Phys.* **2020**, *22*, 17482−17493.
(22) Desiraju, G. R. The C-H···O Hydrogen Bond: Structural Implications and Supramolecular Design. *Acc. Chem. Res.* **1996**, *29*, 441−449.
(23) Shirhatti, P. R.; Maity, D. K.; Wategaonkar, S. C-H···Y Hydrogen Bonds in the Complexes of p-Cresol and p-Cyanophenol with Fluoroform and Chloroform. *J. Phys. Chem. A* **2013**, *117*, 2307−2316.
(24) Ghosh, S.; Wategaonkar, S. C-H···Y (Y = N, O, π) Hydrogen Bond: A Unique Unconventional Hydrogen Bond. *J. Indian Inst. Sci.* **2020**, *100*, 101−125.
(25) Gordy, W.; Stanford, S. C. Spectroscopic Evidence for Hydrogen Bonds: SH, NH and NH2 Compounds. *J. Am. Chem. Soc.* **1940**, *62*, 497−505.
(26) Grzechnik, K.; Rutkowski, K.; Mielke, Z. The S-H N versus O-H N hydrogen bonding in the ammonia complexes with CH_3OH and CH_3SH. *J. Mol. Struct.* **2012**, *1009*, 96−102.
(27) Lobo, I. A.; Robertson, P. A.; Villani, L.; Wilson, D. J. D.; Robertson, E. G. Thiols as Hydrogen Bond Acceptors and Donors: Spectroscopy of 2-Phenylethanethiol Complexes. *J. Phys. Chem. A* **2018**, *122*, 7171−7180.
(28) Forbes, C. R.; Sinha, S. K.; Ganguly, H. K.; Bai, S.; Yap, G. P. A.; Patel, S.; Zondlo, N. J. Insights into Thiol-Aromatic Interactions: A Stereoelectronic Basis for S-H/π Interactions. *J. Am. Chem. Soc.* **2017**, *139*, 1842−1855.
(29) Saggu, M.; Levinson, N. M.; Boxer, S. G. Experimental Quantification of Electrostatics in X-H···π Hydrogen Bonds. *J. Am. Chem. Soc.* **2012**, *134*, 18986−18997.
(30) Biswal, H. S.; Wategaonkar, S. Sulfur, Not Too Far Behind O, N, and C: SH···π Hydrogen Bond. *J. Phys. Chem. A* **2009**, *113*, 12774−12782.
(31) Aarabi, M.; Gholami, S.; Grabowski, S. J. S-H ··· O and O-H ··· O Hydrogen Bonds-Comparison of Dimers of Thiocarboxylic and Carboxylic Acids. *ChemPhysChem* **2020**, *21*, 1653−1664.
(32) Allen, G.; Colclough, R. O. Hydrogen bonding of the thiol group in phosphinodithioic acids. *J. Chem. Soc.* **1957**, 3912−3915.
(33) Boorman, P. M.; Gao, X.; Parvez, M. X-Ray structural characterization of a thiolate salt displaying a very strong S-H S hydrogen bond. *J. Chem. Soc., Chem. Commun.* **1992**, 1656−1658.
(34) Das, A.; Mandal, P. K.; Lovas, F. J.; Medcraft, C.; Walker, N. R.; Arunan, E. The H2S Dimer is Hydrogen-Bonded: Direct Confirmation from Microwave Spectroscopy. *Angew. Chem., Int. Ed.* **2018**, *57*, 15199−15203.
(35) Bhattacherjee, A.; Matsuda, Y.; Fujii, A.; Wategaonkar, S. The Intermolecular S−H···Y (Y = S,O) Hydrogen Bond in the H_2S Dimer and the H_2S-MeOH Complex. *ChemPhysChem* **2013**, *14*, 905−914.
(36) Kemp, W. *Organic spectroscopy*; Macmillan International Higher Education, 2017.
(37) Pavan, M. S.; Sarkar, S.; Row, T. N. G. Exploring the rare S—H S hydrogen bond using charge density analysis in isomers of mercaptobenzoic acid. *Acta Crystallogr., Sect. B: Struct. Sci., Cryst. Eng. Mater.* **2017**, *73*, 626−633.
(38) Steiner, T. S-H···S hydrogen-bond chain in thiosalicylic acid. *Acta Crystallogr., Sect. C: Cryst. Struct. Commun.* **2000**, *56*, 876−877.
(39) Thomas, S. P.; Sathishkumar, R.; Row, T. G. Organic alloys of room temperature liquids thiophenol and selenophenol. *Chem. Commun.* **2015**, *51*, 14255−14258.
(40) Beck, B. W.; Xie, Q.; Ichiye, T. Sequence determination of reduction potentials by cysteinyl hydrogen bonds and peptide dipoles in [4Fe-4S] ferredoxins. *Biophys. J.* **2001**, *81*, 601−613.
(41) Krebs, B. Thio-Compounds and Seleno-Compounds of Main Group Elements - Novel Inorganic Oligomers and Polymers. *Angew. Chem., Int. Ed. Engl.* **1983**, *22*, 113−134.
(42) Gregoret, L. M.; Rader, S. D.; Fletterick, R. J.; Cohen, F. E. Hydrogen bonds involving sulfur atoms in proteins. *Proteins: Struct., Funct., Genet.* **1991**, *9*, 99−107.
(43) Zhou, P.; Tian, F.; Lv, F.; Shang, Z. Geometric characteristics of hydrogen bonds involving sulfur atoms in proteins. *Proteins: Struct., Funct., Genet.* **2009**, *76*, 151−163.
(44) Berman, H. M.; Westbrook, J.; Feng, Z.; Gilliland, G.; Bhat, T. N.; Weissig, H.; Shindyalov, I. N.; Bourne, P. E. The Protein Data Bank. *Nucleic Acids Res.* **2000**, *28*, 235−242.
(45) Word, J. M.; Lovell, S. C.; LaBean, T. H.; Taylor, H. C.; Zalis, M. E.; Presley, B. K.; Richardson, J. S.; Richardson, D. C. Visualizing and quantifying molecular goodness-of-fit: Small-probe contact dots with explicit hydrogen atoms. *J. Mol. Biol.* **1999**, *285*, 1711−1733.
(46) Baker, E. N.; Hubbard, R. E. Hydrogen-Bonding in Globular-Proteins. *Prog. Biophys. Mol. Biol.* **1984**, *44*, 97−179.
(47) Han, S.; You, H. S.; Kim, S.-Y.; Kim, S. K. Dynamic Role of the Intramolecular Hydrogen Bonding in Nonadiabatic Chemistry Revealed in the UV Photodissociation Reactions of 2-Fluorothiophenol and 2-Chlorothiophenol. *J. Phys. Chem. A* **2014**, *118*, 6940−6949.
(48) Ruoff, R. S.; Klots, T. D.; Emilsson, T.; Gutowsky, H. S. Relaxation of Conformers and Isomers in Seeded Supersonic Jets of Inert-Gases. *J. Chem. Phys.* **1990**, *93*, 3142−3150.
(49) Biswal, H. S.; Chakraborty, S.; Wategaonkar, S. Experimental evidence of O-H-S hydrogen bonding in supersonic jet. *J. Chem. Phys.* **2008**, *129*, 184311.
(50) Iwasaki, A.; Fujii, A.; Watanabe, T.; Ebata, T.; Mikami, N. Infrared Spectroscopy of Hydrogen-Bonded Phenol-Amine Clusters in Supersonic Jets. *J. Phys. Chem.* **1996**, *100*, 16053−16057.
(51) Carney, J. R.; Zwier, T. S. Infrared and Ultraviolet Spectroscopy of Water-Containing Clusters of Indole, 1-Methylindole, and 3-Methylindole. *J. Phys. Chem. A* **1999**, *103*, 9943−9957.
(52) Dey, A.; Mondal, S. I.; Sen, S.; Ghosh, D.; Patwari, G. N. Electrostatics determine vibrational frequency shifts in hydrogen bonded complexes. *Phys. Chem. Chem. Phys.* **2014**, *16*, 25247−25250.
(53) Horn, P. R.; Mao, Y.; Head-Gordon, M. Probing non-covalent interactions with a second generation energy decomposition analysis using absolutely localized molecular orbitals. *Phys. Chem. Chem. Phys.* **2016**, *18*, 23067−23079.
(54) Thirman, J.; Engelage, E.; Huber, S. M.; Head-Gordon, M. Characterizing the interplay of Pauli repulsion, electrostatics, dispersion and charge transfer in halogen bonding with energy decomposition analysis. *Phys. Chem. Chem. Phys.* **2018**, *20*, 905−915.
(55) Guerra, C. F.; Bickelhaupt, F. M. Orbital interactions in strong and weak hydrogen bonds are essential for DNA replication. *Angew. Chem., Int. Ed.* **2002**, *41*, 2092−2095.
(56) Kumar, S.; Kaul, I.; Biswas, P.; Das, A. Structure of 7-Azaindole···2-Fluoropyridine Dimer in a Supersonic Jet: Competition between N-H···N and N-H···F Interactions. *J. Phys. Chem. A* **2011**, *115*, 10299−10308.
(57) Kumar, S.; Singh, S. K.; Calabrese, C.; Maris, A.; Melandri, S.; Das, A. Structure of saligenin: microwave, UV and IR spectroscopy studies in a supersonic jet combined with quantum chemistry calculations. *Phys. Chem. Chem. Phys.* **2014**, *16*, 17163−17171.
(58) Das, A.; Mahato, K. K.; Chakraborty, T. Jet spectroscopy of van der Waals dimers of 1-methoxynaphthalene: A laser induced fluorescence study. *J. Chem. Phys.* **2001**, *114*, 8310−8315.
(59) Frisch, M. J.; et al. *Gaussian 09*, Revision D.01; Gaussian, Inc.: Wallingford, CT, 2009.

https://dx.doi.org/10.1021/acs.jpclett.0c03183
J. Phys. Chem. Lett. 2021, 12, 1228−1235

(60) Boys, S. F.; Bernardi, F. The calculation of small molecular interactions by the differences of separate total energies. Some procedures with reduced errors. *Mol. Phys.* **1970**, *19*, 553−566.
(61) Weinhold, F.; Landis, C. R. *Valency and Bonding: A Natural Bond Orbital Donor-Acceptor Perspective*; Cambridge University Press: Cambridge, UK, 2005.
(62) Glendening, E. D.; Landis, C. R.; Weinhold, F. NBO 6.0: Natural bond orbital analysis program. *J. Comput. Chem.* **2013**, *34*, 1429−1437.
(63) Bader, R. F. Atoms in molecules. *Acc. Chem. Res.* **1985**, *18*, 9−15.
(64) Biegler-Konig, F.; Schonbohm, J.; Bayles, D. Software news and updates - AIM2000 - A program to analyze and visualize atoms in molecules. *J. Comput. Chem.* **2001**, *22*, 545−559.
(65) Su, P.; Li, H. Energy decomposition analysis of covalent bonds and intermolecular interactions. *J. Chem. Phys.* **2009**, *131*, 014102.
(66) Khaliullin, R. Z.; Cobar, E. A.; Lochan, R. C.; Bell, A. T.; Head-Gordon, M. Unravelling the Origin of Intermolecular Interactions Using Absolutely Localized Molecular Orbitals. *J. Phys. Chem. A* **2007**, *111*, 8753−8765.
(67) Horn, P. R.; Head-Gordon, M. Polarization contributions to intermolecular interactions revisited with fragment electric-field response functions. *J. Chem. Phys.* **2015**, *143*, 114111.
(68) Schmidt, M. W.; et al. General atomic and molecular electronic structure system. *J. Comput. Chem.* **1993**, *14*, 1347−1363.
(69) Shao, Y.; et al. Advances in molecular quantum chemistry contained in the Q-Chem 4 program package. *Mol. Phys.* **2015**, *113*, 184−215.

https://dx.doi.org/10.1021/acs.jpclett.0c03183
J. Phys. Chem. Lett. 2021, 12, 1228−1235